UDE-based Robust Control for AC/DC Converters

Yeqin Wang
National Wind Institute
Texas Tech University
Lubbock, TX 79409-1021 USA
yeqin.wang@ttu.edu

Yiting Dong, Beibei Ren
Department of Mechanical Engineering
Texas Tech University
Lubbock, TX 79409-1021 USA
yiting.dong@ttu.edu, beibei.ren@ttu.edu

Qing-Chang Zhong
Department of Electrical & Computer Engineering
Illinois Institute of Technology
Chicago, IL 60616 USA
zhongqc@ieee.org

***Abstract*—In this paper, an uncertainty and disturbance estimator (UDE)-based robust control strategy is developed for AC/DC converters to achieve accurate DC-link voltage regulation. The models of both DC-link voltage dynamics and power delivering are derived firstly. The UDE strategy is introduced into both voltage-loop design and power-loop design to handle the uncertainties (e.g., the effects of model/parametric uncertainties), and external disturbances (e.g., variations of both amplitude and frequency in the grid, or load change). The proposed control strategy simplifies the parameter tuning and algorithm implementation, and offers a very robust disturbance rejection capability without additional synchronization units. Simulation results are provided to show the effectiveness of the proposed strategy.**

***Index Terms*—AC/DC converter; DC-link voltage regulation; Uncertainty and disturbance estimator (UDE); Robust control**

I. Introduction

An AC/DC converter is one type of power electronic devices to convert AC power into DC power for different types of DC loads, e.g., batteries, LEDs, DC motors, digital devices, and plays an important role in power systems [1]–[4]. For an ideal AC/DC converter, it is expected that the output voltage is a pure DC signal without any oscillation. Many AC/DC converters use diode rectifiers cascaded with a boost converter, but the power flow is unidirectional from the AC side to the load, and the reactive power usually cannot be well regulated either. Therefore, many control strategies are developed for AC/DC converters to achieve accurate DC-link output voltage regulation with unity power factor operation [5], [6].

The cascaded control methods are commonly used for AC/DC converters with an external voltage-loop and an inner current-loop [1]. The external voltage-loop is usually a proportional-integral (PI) controller to regulate the DC-link voltage and to generate a current reference for the inner loop, while the inner loop is used to regulate the AC current to track the current reference. There exist many control strategies for inner current-loop design to facilitate the accurate DC-link voltage regulation. The most widely used control strategy is the voltage oriented control, which can offer both good static and dynamic performance for AC/DC converters with the high bandwidth current controller [7]. Also, the inner loop can be used for over-current protection [8], [9]. In order to achieve a higher robustness and better output performance, some artificial intelligent techniques are incorporated with the inner current-loop design, such as neural networks [10], [11] and fuzzy logic systems [12], [13].

In the current-loop design, in order to provide the phase and frequency information of the utility grid, and to generate a AC current reference, a dedicated synchronization unit is usually required. Currently, the most commonly synchronization method is the phase-locked loop (PLL) [14]. However, since the PLL dynamics is highly nonlinear, it is inevitable that the stability of converters will be affected by PLL dynamics, especially in the weak grid [15]. Besides, the slow PLL response may directly limit the control performance, and it is time-consuming and difficult to choose the PLL parameters to realize a prospective performance [16].

In order to remove the effect from the PLL, power-based control strategy has been introduced into the control of AC/DC converters [17]. It still consists of an external voltage-loop to generate a desired power reference, and an inner power-loop with power flow control to facilitate the accurate DC-link voltage regulation. And the power loop can achieve accurate power delivery from the utility grid to the DC-link. In [18], although the power reference is generated in the voltage-loop design, the core part of power control is essentially the current-based control. Since the power reference is transferred into the current reference in [18], the proportional-resonant control method is used for current control in $\alpha - \beta$ reference frame. Though the synchronization unit is removed in [18], the current reference is generated through the division between power reference and grid voltage in $\alpha - \beta$ reference frame. The robustness might not be guaranteed if the large disturbances happen in grid side. In [17], the power control with synchronverter technology is adopted for AC/DC converters to control the DC-link output voltage. However, the whole control loop is still based on the traditional PI controller or integral controller.

The robust control for both DC-link voltage regulation and power regulation is important for AC/DC converters. However, the DC-link dynamics is highly affected by real power disturbance and load change. Furthermore, the AC/DC converter is inherently nonlinear, which is a big challenge for power-loop design. In this paper, in order to improve the performance in the presence of uncertainties and disturbances, a robust control strategy based on the uncertainty and disturbance estimator (UDE) technology is introduced for AC/DC converters to accurately regulate the output DC voltage with flexible control

978-1-5090-6684-1/18/$31.00 ©2018 IEEE

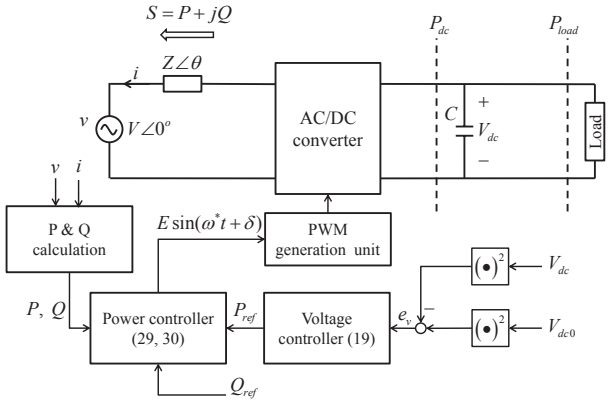

Fig. 1. An AC/DC converter with the proposed control strategy.

of the reactive power. Recently, the utilization of UDE-based control strategy [19] for estimating and compensating the external disturbance has gained much attention. Many UDE-based research results have been developed for uncertain and nonlinear systems [20], and broad applications, including power electronics control [21], renewables [22], [23], etc.

Given the above analysis, the objective of this paper is to develop the UDE-based robust control strategy for AC/DC converters. The models of both DC-link voltage dynamics and power delivering are derived firstly, and the UDE technology is developed in both voltage-loop design and power-loop design. The main contributions of the paper lie in:

- The proposed power-based control method consists of an external voltage-loop to generate a desired power reference, and an inner power-loop to directly regulate the power delivery from the utility grid to the DC-link. The presented control strategy can achieve accurate DC-link output voltage regulation, without an additional synchronization unit or the measurement of load power.
- The UDE technology is incorporated with the proposed power-based control strategy, which offers high robustness and fast dynamic response against uncertainties, disturbances, and load change.

The rest of this paper is organized as follows. Section II provides the dynamics of AC/DC converters, and formulates the control problem. In Section III, the UDE-based robust controllers are developed with the closed-loop system stability analysis. Section IV demonstrates the performance of the proposed method by simulation studies. The last section concludes the paper.

II. Problem Formulation and Preliminaries

Fig. 1 shows the circuit of an AC/DC converter with the proposed control strategy. The details of modeling are firstly provided as follows.

A. DC-Link Voltage Dynamics

The DC-link power balance shown in Fig. 1 can be obtained as

$$\frac{d}{dt}\left(\frac{1}{2}CV_{dc}^2\right) = P_{dc} - P_{load}, \tag{1}$$

where C is the capacitance of the capacitor, V_{dc} is the DC-link voltage, P_{dc} is the DC power from the AC/DC converter, P_{load} is the load power which is treated as unknown and varying. The power balance in the AC/DC converter is calculated as

$$-P = P_{loss} + P_{dc}, \tag{2}$$

where P is AC real power from the AC/DC converter to the grid, and P_{loss} is the total power losses, e.g., the power losses on power electronics or parasitic resistance. Substituting (2) into (1), the DC-link dynamics can be finally obtained as

$$\frac{d}{dt}\left(\frac{1}{2}CV_{dc}^2\right) = -P + \Delta_{dc}, \tag{3}$$

where

$$\Delta_{dc} = -P_{loss} - P_{load}, \tag{4}$$

represents the lumped uncertain term.

B. The Modeling of Power Delivering

Since an AC/DC converter can be operated as a bidirectional converter, in this paper, the power S is formulated from the voltage source $E\angle\delta$ to the grid $V\angle 0^o$. The real power P and the reactive power Q are

$$P = \left(\frac{EV}{Z}\cos\delta - \frac{V^2}{Z}\right)\cos\theta + \frac{EV}{Z}\sin\delta\sin\theta, \tag{5}$$

$$Q = \left(\frac{EV}{Z}\cos\delta - \frac{V^2}{Z}\right)\sin\theta - \frac{EV}{Z}\sin\delta\cos\theta, \tag{6}$$

where δ is the power angle. Taking the time derivative of both (5) and (6), it yields [21]

$$\begin{aligned}\dot{P} &= \frac{EV\dot{\delta}}{Z}\cos\delta\sin\theta - \frac{EV\dot{\delta}}{Z}\sin\delta\cos\theta \\ &\quad + \frac{V\dot{E}}{Z}\cos\delta\cos\theta + \frac{V\dot{E}}{Z}\sin\delta\sin\theta,\end{aligned} \tag{7}$$

$$\begin{aligned}\dot{Q} &= \frac{V\dot{E}}{Z}\cos\delta\sin\theta - \frac{EV\dot{\delta}}{Z}\sin\delta\sin\theta \\ &\quad - \frac{EV\dot{\delta}}{Z}\cos\delta\cos\theta - \frac{V\dot{E}}{Z}\sin\delta\cos\theta.\end{aligned} \tag{8}$$

In practice, the output impedance is mostly inductive, which means $\sin\theta \approx 1$ and $\cos\theta \approx 0$. Furthermore, the power angle δ is usually very small with $\sin\delta \approx 0$ and $\cos\delta \approx 1$. Thus, the power flow dynamics (7) and (8) can be re-written as

$$\dot{P} = \frac{EV}{Z_o}\dot{\delta} + \Delta_p, \tag{9}$$

$$\dot{Q} = \frac{V}{Z_o}\dot{E} + \Delta_q, \tag{10}$$

where

$$\begin{aligned}\Delta_p &= -\frac{EV\dot{\delta}}{Z_o}\sin\delta\cos\theta + \frac{EV\dot{\delta}}{Z_o}(\cos\delta\sin\theta - 1) \\ &\quad + \frac{V\dot{E}}{Z_o}\sin\delta\sin\theta + \frac{V\dot{E}}{Z_o}\cos\delta\cos\theta + d_p,\end{aligned} \tag{11}$$

$$\Delta_q = -\frac{EV\dot{\delta}}{Z_o}\sin\delta\sin\theta + \frac{V\dot{E}}{Z_o}(\cos\delta\sin\theta - 1)$$

$$-\frac{V\dot{E}}{Z_o}\sin\delta\cos\theta-\frac{EV\dot{\delta}}{Z_o}\cos\delta\cos\theta+d_q, \quad (12)$$

represent the lumped uncertain terms, with d_p and d_q being the deviations due to the mismatches between the real impedance Z in (7) and (8) and the nominal impedance Z_o.

III. Robust Control Design and Stability Analysis

The control objective of AC/DC converters is to achieve accurate DC-link voltage regulation, i.e., the DC-link voltage V_{dc} can accurately track the reference V_{dc0}. As shown in Fig. 1, the cascaded control design, where the voltage control is to regulate DC-link voltage and to generate a desired power reference, while the power control is to achieve accurate power delivery and facilitate DC-link voltage regulation, is proposed with the incorporation of the UDE-based robust control strategy. It is worth noting that the reactive power can be flexibly regulated with the artificial setting of the reactive power reference Q_{ref}.

A. Voltage Control Design

The aim of voltage control is to generate a desired power reference P_{ref} for the power-loop design, and then to regulate the output voltage V_{dc} asymptotically track the voltage reference V_{dc0}. The tracking error is defined as

$$e_v=(V_{dc0})^2-V_{dc}^2, \quad (13)$$

which satisfies the desired error dynamics as

$$\dot{e}_v=-k_v e_v, \quad (14)$$

where $k_v>0$ is the error feedback control gain. Combining (3) and (14), it yields

$$P_{ref}=-CV_{dc0}\dot{V}_{dc0}-\frac{C}{2}k_v e_v+\Delta_{dc}. \quad (15)$$

According to the DC-link voltage dynamics (3), the uncertain term Δ_{dc} can be obtained as

$$\Delta_{dc}=P_{ref}+\frac{d}{dt}\left(\frac{1}{2}CV_{dc}^2\right). \quad (16)$$

Following the UDE procedure provided in [19], Δ_{dc} can be estimated by

$$\hat{\Delta}_{dc}=g_{vf}*\Delta_{dc}=g_{vf}*\left[P_{ref}+\frac{d}{dt}\left(\frac{1}{2}CV_{dc}^2\right)\right], \quad (17)$$

where g_{vf} is the impulse response of a strictly proper stable filter $G_{vf}(s)$ with the appropriate bandwidth, and $*$ is the convolution operator. Replacing Δ_{dc} with $\hat{\Delta}_{dc}$ in (15) results in

$$\begin{aligned}P_{ref} &= -CV_{dc0}\dot{V}_{dc0}+g_{vf}*\left[P_{ref}+\frac{d}{dt}\left(\frac{1}{2}CV_{dc}^2\right)\right]\\ &\quad -\frac{C}{2}k_v e_v. \end{aligned}\quad (18)$$

Then, the UDE-based virtual control input P_{ref} can be formulated as

$$\begin{aligned}P_{ref} &= L^{-1}\left\{\frac{1}{1-G_{vf}(s)}\right\}*\left(-CV_{dc0}\dot{V}_{dc0}-\frac{C}{2}k_v e_v\right)\\ &\quad -L^{-1}\left\{\frac{sG_{vf}(s)}{1-G_{vf}(s)}\right\}*\left(\frac{1}{2}CV_{dc}^2\right). \end{aligned}\quad (19)$$

B. Power Control Design

The aim of power control is to achieve accurate power delivery between the utility grid and AC/DC converters, such that both P and Q can track their settings P_{ref} and Q_{ref}, respectively. The tracking error signals are defined as

$$e_p=P_{ref}-P, \quad e_q=Q_{ref}-Q, \quad (20)$$

where P_{ref} is the power reference from the previous subsection, and Q_{ref} is the artificial reactive power reference which usually can be set as 0 to keep unity power factor. The error signal (20) should satisfy the desired error dynamics as

$$\dot{e}_p=-k_p e_p, \quad \dot{e}_q=-k_q e_q, \quad (21)$$

where k_p and k_q are error feedback control gains. Substituting (9)-(10) into (21), respectively, it yields

$$\dot{\delta} = \frac{Z_o}{EV}\left(\dot{P}_{ref}+k_p e_p-\Delta_p\right), \quad (22)$$

$$\dot{E} = \frac{Z_o}{V}\left(\dot{Q}_{ref}+k_q e_q-\Delta_q\right). \quad (23)$$

According to the power flow dynamics in (9) and (10), the uncertain terms Δ_p and Δ_q can be expressed as

$$\Delta_p=-\frac{EV}{Z_o}\dot{\delta}+\dot{P}, \quad \Delta_q=-\frac{V}{Z_o}\dot{E}+\dot{Q}. \quad (24)$$

Following the UDE procedure provided in [19], the uncertain terms Δ_p and Δ_q can be estimated by

$$\hat{\Delta}_p = g_{pf}*\left(-\frac{EV}{Z_o}\dot{\delta}+\dot{P}\right), \quad (25)$$

$$\hat{\Delta}_q = g_{qf}*\left(-\frac{V}{Z_o}\dot{E}+\dot{Q}\right), \quad (26)$$

where g_{pf} and g_{qf} are impulse responses of strictly proper stable filters $G_{pf}(s)$ and $G_{qf}(s)$ with the appropriate bandwidth, respectively. Replacing Δ_p with $\hat{\Delta}_p$ in (22) and Δ_q with $\hat{\Delta}_q$ in (23) yield

$$\dot{\delta} = \frac{Z_o}{EV}\left[\dot{P}_{ref}-g_{pf}*\left(\dot{P}-\frac{EV}{Z_o}\dot{\delta}\right)+k_p e_p\right], \quad (27)$$

$$\dot{E} = \frac{Z_o}{V}\left[\dot{Q}_{ref}-g_{qf}*\left(\dot{Q}-\frac{V}{Z_o}\dot{E}\right)+k_q e_q\right]. \quad (28)$$

Then, the power control laws are obtained as

$$\begin{aligned}\dot{\delta} &= \frac{Z_o}{EV}\left[L^{-1}\left\{\frac{1}{1-G_{pf}(s)}\right\}*\left(\dot{P}_{ref}+k_p e_p\right)\right]\\ &\quad -\frac{Z_o}{EV}\left[L^{-1}\left\{\frac{sG_{pf}(s)}{1-G_{pf}(s)}\right\}*P\right], \end{aligned}\quad (29)$$

$$\begin{aligned}\dot{E} &= \frac{Z_o}{V}\left[L^{-1}\left\{\frac{1}{1-G_{qf}(s)}\right\}*\left(\dot{Q}_{ref}+k_q e_q\right)\right]\\ &\quad -\frac{Z_o}{V}\left[L^{-1}\left\{\frac{sG_{qf}(s)}{1-G_{qf}(s)}\right\}*Q\right]. \end{aligned}\quad (30)$$

The final control signal $E\sin(\omega^* t+\delta)$ for generating the pulse width modulation (PWM) signal can be obtained after

combining the amplitude E and the frequency from the phase δ, where ω^* is the rated frequency for global settings.

C. Stability Analysis

The stability analysis of AC/DC converters is given by the following theorem.

Theorem 1: Consider the model of AC/DC converters described by DC-link voltage dynamics (3), and power flow dynamics (9) and (10), the UDE-based control strategy consisting of voltage controller (19), and power controllers (29) and (30). If the filters $G_{vf}(s)$, $G_{pf}(s)$ and $G_{qf}(s)$ are chosen appropriately as strictly proper stable filters with unity gain and zero phase shift over the spectrum of the uncertainty and zero gain elsewhere, it can be concluded that all signals in the closed-loop system are uniformly bounded. Furthermore, the error signals e_v, e_p and e_q converge uniformly to compact sets Ω_{ev}, Ω_{ep} and Ω_{eq} as defined in (31)-(33), whose sizes can be reduced by appropriately choosing the control gains and designing the filters, i.e.,

$$\Omega_{ev}: = \left\{ e_v \in \mathbb{R} | \ \|e_v\| \leq \sqrt{\frac{4}{C}\left[V(0)+\frac{c}{\rho}\right]} \right\}, \quad (31)$$

$$\Omega_{ep}: = \left\{ e_p \in \mathbb{R} | \ \|e_p\| \leq \sqrt{2\left[V(0)+\frac{c}{\rho}\right]} \right\}, \quad (32)$$

$$\Omega_{eq}: = \left\{ e_q \in \mathbb{R} | \ \|e_q\| \leq \sqrt{2\left[V(0)+\frac{c}{\rho}\right]} \right\}, \quad (33)$$

where $V(0)$ is the initial value of V defined by (34), $\rho = \min\{2k_v - 2/C,\ 2k_p - 1,\ 2k_q - 1\}$ and $c = 0.5\left(\|\tilde{\Delta}_{dc}\|^2 + \|\tilde{\Delta}_p\|^2 + \|\tilde{\Delta}_q\|^2\right)$.

Proof: Consider the following Lyapunov function candidate

$$V = \frac{C}{4}e_v^2 + \frac{1}{2}e_p^2 + \frac{1}{2}e_q^2. \quad (34)$$

Taking the time derivative of V along with the UDE-based control laws (19), (29) and (30) yields

$$\dot{V} = -\frac{C}{2}k_v e_v^2 - k_p e_p^2 - k_q e_q^2 - e_v\tilde{\Delta}_{dc} + e_p\tilde{\Delta}_p + e_q\tilde{\Delta}_q, \quad (35)$$

where $\tilde{\Delta}_{dc} = \hat{\Delta}_{dc} - \Delta_{dc}$, $\tilde{\Delta}_p = \hat{\Delta}_p - \Delta_p$ and $\tilde{\Delta}_q = \hat{\Delta}_q - \Delta_q$ are estimation errors with $\tilde{\Delta}_{dc} = \Delta_{dc} * L^{-1}\{1 - G_{vf}(s)\}$, $\tilde{\Delta}_p = \Delta_p * L^{-1}\{1 - G_{pf}(s)\}$ and $\tilde{\Delta}_q = \Delta_q * L^{-1}\{1 - G_{qf}(s)\}$. Assume that those terms Δ_{dc}, Δ_p and Δ_q are bounded, the estimation errors $\tilde{\Delta}_{dc}$, $\tilde{\Delta}_p$ and $\tilde{\Delta}_p$ are also bounded. By using Young's inequality, it can be easily obtained as

$$\dot{V} \leq -\rho V + c, \quad (36)$$

where $\rho = \min\{2k_v - 2/C,\ 2k_p - 1,\ 2k_q - 1\}$ and $c = 0.5\left(\|\tilde{\Delta}_{dc}\|^2 + \|\tilde{\Delta}_p\|^2 + \|\tilde{\Delta}_q\|^2\right)$. To ensure $\rho > 0$, the control parameters k_v, k_p and k_q are chosen to satisfy the following conditions: $2k_v - 2/C > 0$, $2k_p - 1 > 0$ and $2k_q - 1 > 0$. From the above analysis, it is straightforward to show that the signals e_v, e_p and e_q are uniformly bounded. Especially, multiplying (36) by $e^{\rho t}$ and then integrating the inequality yields $V \leq V(0) + c/\rho$, which implies that $\|e_v\| \leq \sqrt{\frac{4}{C}\left[V(0)+\frac{c}{\rho}\right]}$, $\|e_p\| \leq \sqrt{2\left[V(0)+\frac{c}{\rho}\right]}$ and $\|e_q\| \leq \sqrt{2\left[V(0)+\frac{c}{\rho}\right]}$. Hence, e_v, e_p and e_q converge to the compact sets Ω_{ev}, Ω_{ep} and Ω_{eq}, respectively. This concludes the proof.■

TABLE I
SYSTEM PARAMETERS

Parameter	Value	Parameter	Value
L	2.2 mH	R	$30 \sim 50\,\Omega$
r	$0.5\,\Omega$	Normal grid voltage	$24\,V_{rms}$
C	1950 uF	Normal grid frequency	60 Hz

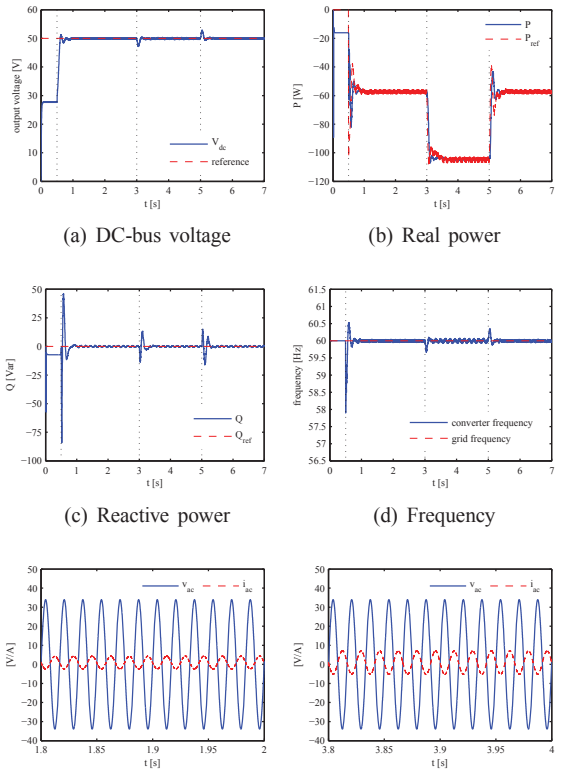

(a) DC-bus voltage (b) Real power

(c) Reactive power (d) Frequency

(e) Instantaneous voltage and current when $t \in [1.8,\ 2]$ (f) Instantaneous voltage and current when $t \in [3.8,\ 4.0]$

Fig. 2. Simulation results with load change

IV. Simulation Studies

In order to verify the effectiveness of the proposed controller, simulations are carried out in MATLAB/Simulink/SimpowerSystems, with the solvers ode45t and the sampling time of 1×10^{-6}s. A single-phase AC/DC converter is used as a simulation example, and the PWM operation frequency is set as 20 kHz. The system parameters are given in Table I, with the impedance Z consisting of a resistor r and an inductor L, and R being the load.

The feedback gains are chosen with $k_v = 600$, $k_p = 150$, $k_q = 200$ and $Z_o = \sqrt{(2\pi fL)^2 + r^2}$. The desired DC-link output voltage is set as $V_{dc0} = 50V$, and the reactive

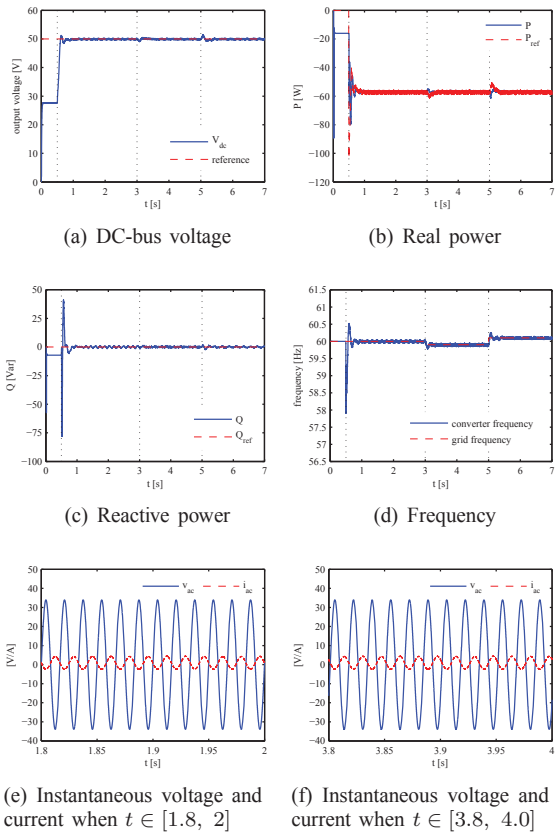

(a) DC-bus voltage (b) Real power

(c) Reactive power (d) Frequency

(e) Instantaneous voltage and current when $t \in [1.8,\ 2]$ (f) Instantaneous voltage and current when $t \in [3.8,\ 4.0]$

Fig. 3. Simulation results with grid frequency change

power reference Q_{ref} is set as 0. According to the guidance of filter design in [21], [24], the UDE filters are chosen as $G_{vf}(s) = \frac{1}{(0.05s)^2+\sqrt{2}\times 0.05s+1}$, $G_{pf}(s) = \frac{1}{(0.1s)^2+\sqrt{2}\times 0.1s+1}$ and $G_{qf}(s) = \frac{1}{(0.05s)^2+\sqrt{2}\times 0.05s+1}$.

A. Case 1: Operation with load change

The simulation starts at $t = 0$. The initial synchronization is achieved during the first 0.5 second. During this period, the AC/DC converter works as an uncontrolled rectifier supplying a load R of 50Ω. This allowed the internal frequency to synchronize with the frequency of the grid. At $t = 0.5$s, the PWM signal is enabled. The DC-bus voltage increases and settles at the reference value 50V, without overshoot, as shown in Fig. 2(a). This is due to the fast dynamic response of the proposed UDE-based robust controller. The real power converges to a constant, and the reactive power is regulated to zero after some transients, shown in Figs. 2(b) and 2(c) respectively. Although there exist some weak oscillations in Figs. 2(b) and 2(c), the proposed UDE-based DC-link voltage controller can handle those weak oscillations and make the DC-link output voltage smooth, as shown in Fig. 2(a). At $t = 3$s, the load is changed to $R = 30\Omega$. From Fig. 2(a), the DC-link voltage is regulated well after some undershoot transients. Those undershoot transients are caused by the sudden increased load. However, the output voltage can converge to the voltage reference at 50V immediately with the help of the proposed controller. Besides, because of the increased load, the real power increases at about 100W shown in Fig. 2(b), while the reactive power goes through some transients but settles down at zero again. At $t = 5$s, the load is returned to $R = 50\Omega$. Although the increased load causes the overshoot, the DC-link voltage is also regulated well at 50V in Fig. 2(a). During the whole process, the internal frequency autonomously synchronizes with the grid frequency all the time, except some expected transients, shown as Fig. 2(d). The zoomed-in instantaneous voltage and current on AC side are given by Figs. 2(e) and 2(f). It can be observed that the phase difference between the voltage and the current is 180^o, which means negative real power and unity power factor are achieved by the proposed controller, and the power is delivered from the AC grid to the load.

B. Case 2: Operation with grid frequency change

In Case 2, the effect of grid frequency change is investigated to verify the robustness of the proposed control method. Similarly to Case 1, the control is enabled at $t = 0.5$s with the grid frequency as 60Hz. The output voltage can converge to the reference 50V shown in Fig. 3(a). At $t = 3$s, the grid frequency drops from 60Hz to 59.9Hz. However, the DC-link output voltage is still regulated well with few oscillations in Fig. 3(a). This is because the proposed control has a strong capability to autonomously track the grid frequency. The real power and reactive power can also settle down quickly in Figs. 3(b) and 3(c), since the UDE-based power controller has a strong robustness against the grid frequency changes. At $t = 5$s, the grid frequency increases from 59.9Hz to 60.1Hz. The DC-link voltage can be well regulated at 50V as well, which is given by Fig. 3(a). As shown in Figs. 3(b) and 3(c), the real power and reactive power can be regulated with the proposed controller. From Fig. 3(d), it can be easily observed that the converter frequency autonomously synchronizes with the grid frequency well without the PLL. The zoomed-in instantaneous voltage and current are shown in Figs. 3(e) and 3(f).

C. Case 3: Operation with grid voltage dip

In order to further test the robustness of the proposed controller, the case of voltage dips at the grid voltage is investigated. Similarly to Case 1, the proposed control is enabled at $t = 0.5$s. From Fig. 4(a), it can be observed that the DC-link voltage increases and settles at $50V$. The real power converges to a constant, and the reactive power is regulated to zero after some transients, shown in Figs. 4(b) and 4(c) respectively. At $t = 3$s, the RMS grid voltage drops from 24V to 21.6V, which corresponds to a 10% voltage drop. However, the DC-link voltage is regulated well after some transients. From Figs. 4(b) and 4(c), there exist some oscillations at $t = 3$s, which is caused by the grid voltage dips. However, the real power and reactive power can settle down with fast response. At $t = 5$s, the RMS grid voltage returns to 24V. The output voltage is also regulated well at 50V. Fig. 4(d) shows that the converter RMS voltage tracks the grid RMS voltage well. Although there exists an overshoot initially, which is

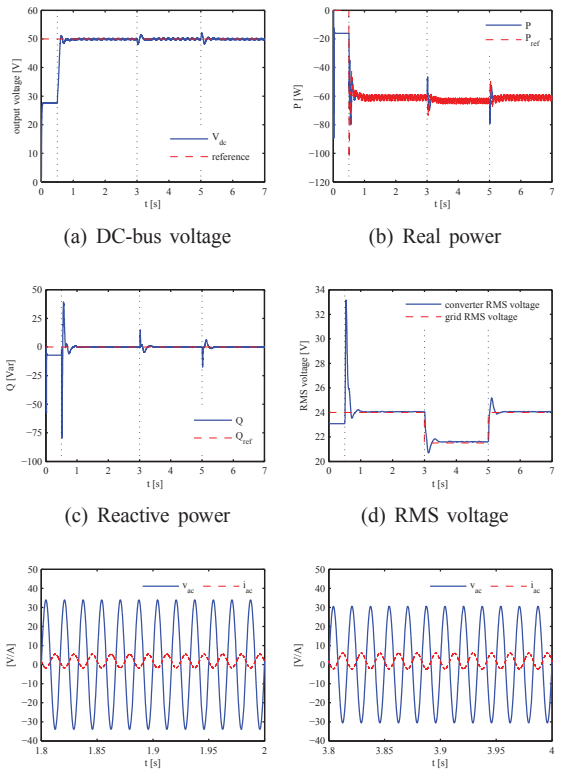

(a) DC-bus voltage (b) Real power

(c) Reactive power (d) RMS voltage

(e) Instantaneous voltage and current when $t \in [1.8\ 2]$ (f) Instantaneous voltage and current when $t \in [3.8\ 4.0]$

Fig. 4. Simulation results with grid voltage change

caused by the initial error, the converter RMS voltage can follow the grid RMS voltage with fast dynamic response. The zoomed-in instantaneous voltage and current on AC side are given by Figs. 4(e) and 4(f).

V. Conclusion

The UDE-based robust control has been developed for AC/DC converters to accurately regulate the DC-link voltage in this paper. Both power flow dynamics and DC-link voltage dynamics have been included in the dynamic model of AC/DC converters. The UDE method has been employed for both voltage control and power control to deal with the model uncertainties and external disturbances, without any extra PLL synchronization unit. The effectiveness of the proposed strategy has been validated under different simulation scenarios.

References

[1] Q.-C. Zhong and T. Hornik, *Control of Power Inverters in Renewable Energy and Smart Grid Integration*. New York, NJ, USA: Wiley-IEEE Press, 2013.

[2] M. P. Bahrman and B. K. Johnson, "The ABCs of HVDC transmission technologies," *IEEE power and energy magazine*, vol. 5, no. 2, pp. 32–44, 2007.

[3] J. G. Hwang, P. W. Lehn, and M. Winkelnkemper, "A generalized class of stationary frame-current controllers for grid-connected AC–DC converters," *IEEE Trans. Power Del.*, vol. 25, no. 4, pp. 2742–2751, 2010.

[4] B.-Y. Chen and Y.-S. Lai, "Switching control technique of phase-shift-controlled full-bridge converter to improve efficiency under light-load and standby conditions without additional auxiliary components," *IEEE Trans. Power Electron.*, vol. 25, no. 4, pp. 1001–1012, 2010.

[5] M. Cichowlas, M. Malinowski, M. P. Kazmierkowski, D. L. Sobczuk, P. Rodríguez, and J. Pou, "Active filtering function of three-phase PWM boost rectifier under different line voltage conditions," *IEEE Trans. Ind. Electron.*, vol. 52, no. 2, pp. 410–419, 2005.

[6] J. R. Rodríguez, J. W. Dixon, J. R. Espinoza, J. Pontt, and P. Lezana, "PWM regenerative rectifiers: State of the art," *IEEE Trans. Ind. Electron.*, vol. 52, no. 1, pp. 5–22, 2005.

[7] K. Zhou and D. Wang, "Digital repetitive controlled three-phase PWM rectifier," *IEEE Trans. Power Electron.*, vol. 18, no. 1, pp. 309–316, 2003.

[8] A. Dell'Aquila, M. Liserre, V. G. Monopoli, and P. Rotondo, "Overview of PI-based solutions for the control of DC buses of a single-phase H-bridge multilevel active rectifier," *IEEE Trans. Ind. Appl.*, vol. 44, no. 3, pp. 857–866, 2008.

[9] O. Kukrer, H. Komurcugil, and A. Doganalp, "A three-level hysteresis function approach to the sliding-mode control of single-phase UPS inverters," *IEEE Trans. Ind. Electron.*, vol. 56, no. 9, pp. 3477–3486, 2009.

[10] F. Kamran, R. G. Harley, B. Burton, T. G. Habetler, and M. A. Brooke, "A fast on-line neural-network training algorithm for a rectifier regulator," *IEEE Trans. Power Electron.*, vol. 13, no. 2, pp. 366–371, 1998.

[11] B. K. Bose, "Neural network applications in power electronics and motor drivesłan introduction and perspective," *IEEE Trans. Ind. Electron.*, vol. 54, no. 1, pp. 14–33, 2007.

[12] C. Cecati, A. Dell'Aquila, A. Lecci, and M. Liserre, "Implementation issues of a fuzzy-logic-based three-phase active rectifier employing only voltage sensors," *IEEE Trans. Ind. Electron.*, vol. 52, no. 2, pp. 378–385, 2005.

[13] A. Bouafia, F. Krim, and J.-P. Gaubert, "Fuzzy-logic-based switching state selection for direct power control of three-phase PWM rectifier," *IEEE Trans. Ind. Electron.*, vol. 56, no. 6, pp. 1984–1992, 2009.

[14] M. Karimi-Ghartemani and M. R. Iravani, "A nonlinear adaptive filter for online signal analysis in power systems: Applications," *IEEE Trans. Power Del.*, vol. 17, no. 2, pp. 617–622, 2002.

[15] M. Ashabani and Y. A.-R. I. Mohamed, "Novel comprehensive control framework for incorporating VSCs to smart power grids using bidirectional synchronous-VSC," *IEEE Trans. Power Syst.*, vol. 29, no. 2, pp. 943–957, 2014.

[16] Q.-C. Zhong, P.-L. Nguyen, Z. Ma, and W. Sheng, "Self-synchronised synchronverters: Inverters without a dedicated synchronisation unit," *IEEE Trans. Power Electron.*, vol. 29, no. 2, pp. 617–630, Feb. 2014.

[17] Z. Ma, Q.-C. Zhong, and J. Yan, "Synchronverter-based control strategies for three-phase PWM rectifiers," in *Proc. of the 7th IEEE Conference on Industrial Electronics and Applications (ICIEA)*, Singapore, Jul. 2012.

[18] J. Lu, S. Golestan, M. Savaghebi, J. C. Vasquez, J. M. Guerrero, and A. Marzabal, "An Enhanced State Observer for DC-Link Voltage Control of Three-Phase AC/DC Converters," *IEEE Trans. Power Electron.*, vol. 33, no. 2, pp. 936–942, 2018.

[19] Q.-C. Zhong and D. Rees, "Control of uncertain LTI systems based on an uncertainty and disturbance estimator," *ASME Trans. J. Dyn. Sys. Meas. Control*, vol. 126, no. 4, pp. 905–910, Dec. 2004.

[20] R. K. Stobart and Q.-C. Zhong, "Uncertainty and disturbance estimator-based control for uncertain LTI-SISO systems with state delays," *ASME Trans. J. Dyn. Sys. Meas. Control*, vol. 133, no. 2, pp. 1–6, 2011.

[21] Y. Wang, B. Ren, and Q.-C. Zhong, "Robust power flow control of grid-connected inverters," *IEEE Trans. Ind. Electron.*, vol. 63, no. 11, pp. 6887–6897, Nov. 2016.

[22] B. Ren, Y. Wang, and Q.-C. Zhong, "UDE-based control of variable-speed wind turbine systems," *International Journal of Control*, vol. 90, no. 1, pp. 121–136, Jan. 2017.

[23] Y. Wang and B. Ren, "Fault ride-through enhancement for grid-tied PV systems with robust control," *IEEE Trans. Ind. Electron.*, vol. 65, no. 3, pp. 2302–2312, Mar 2018.

[24] B. Ren, Q.-C. Zhong, and J. Dai, "Asymptotic reference tracking and disturbance rejection of UDE-based robust control," *IEEE Trans. Ind. Electron.*, vol. 64, no. 4, pp. 3166–3176, Apr. 2017.